

# Effects of Implantation Heating on Exfoliation of InP

Sumiko Hayashi\*, Rajinder Sandhu<sup>1</sup>, David Bruno, Mike Wojtowicz<sup>1</sup>  
and Mark S. Goorsky

Department of Materials Science and Engineering  
University of California, Los Angeles, CA 90095, USA  
<sup>1</sup>Northrop Grumman Space Technology,  
Redondo Beach, CA 90278, USA

(Received December 2, 2004; accepted May 13, 2005)

**Key words:** ion implantation, InP, high resolution X-ray diffraction, defects

The effect of self-heating during 150 keV hydrogen implantation at a dose of 2.5 and  $5 \times 10^{16}$  H<sub>2</sub><sup>+</sup>/cm<sup>2</sup> on the exfoliation of InP is investigated. For material implanted without controlled cooling, significant heating during the implantation prevented subsequent layer transfer. The failure to exfoliate the layer in this case is attributed to the loss of hydrogen and the inability to form platelet type defects at a high temperature. Additionally, the damage profile observed by transmission electron microscopy in the uncooled sample extends from the projected range to the surface of the substrate. In contrast, the implant damage and defects of InP cooled to  $-20^\circ\text{C}$  are well confined to a single layer at the projected range with a thickness of about 150 nm. This thinner damage distribution is believed to be able to trap more effectively the hydrogen. This in turn, allows greater coalescence of the hydrogen and the platelet defects leading to exfoliation. The successful exfoliation of III-V materials is more sensitive to implant conditions than in the case of Si possibly due to the significantly lower thermal conductivity in III-Vs, which will ultimately lead to greater target heating during implantation.

## 1. Introduction

The success of silicon-on-insulator fabrication by wafer bonding and layer transfer techniques gives a promising outlook for the integration of other material systems. For a variety of III-V applications, conventional epitaxial techniques are not adequate due to a large lattice mismatch; however, wafer bonding offers a suitable alternative.<sup>(1,2)</sup> In particular, the technique of hydrogen implantation and exfoliation is attractive due to the high cost of bulk III-V materials. In this process, a high dose of hydrogen is implanted into the

---

\*Corresponding author, e-mail address: sumiko@seas.ucla.edu

substrate and upon annealing hydrogen-filled platelets form and coalesce to induce the exfoliation of a thin layer.<sup>(3,4)</sup> The bulk of the substrate is virtually unaffected and may be recycled to produce multiple exfoliation layers.

The hydrogen splitting of a variety of III-V materials has been reported; however, several reports indicate that thermal history during and after implantation is critical to the formation of exfoliation-inducing defects.<sup>(4-7)</sup> For example, with InP, an implantation temperature or subsequent annealing temperature of 150–250°C is required to form the platelet defects necessary for layer exfoliation.<sup>(6,7)</sup> Additionally, it has been reported that for Si the thickness and morphology of the transferred layer can be varied by the temperature at which implantation takes place.<sup>(8)</sup> In that study, implantation at room temperature led to narrower damage profiles (thicker layers) and smoother exfoliated surfaces than implantation at –140°C. In this study, the effect of implantation temperature on InP was investigated. Two implantation samples were investigated; one that was implanted at room temperature and another where the target was cooled to nominally –20°C to determine its effect on subsequent exfoliation.

## 2. Experiment

Three-inch Fe-doped semi-insulating ( $10^7 \Omega\text{cm}$ ) InP substrates were exposed to solvent cleaning and then coated with 800 Å of SiN. The SiN was then out-gassed at 500°C for 1 min in nitrogen before implantation. Two sets of implantation runs were completed. In one case, the substrate was implanted at room temperature without any active cooling of the substrate. In the second case, the substrate was bonded to a Si carrier wafer with silver paste to achieve efficient, uniform cooling to –20°C. Implantation of  $\text{H}_2^+$  was performed at 150 keV. Two doses were implanted for each set of runs:  $2.5 \times 10^{16}$  and  $5.0 \times 10^{16} \text{H}_2^+/\text{cm}^2$ . The beam current for all of the implantations was kept at approximately 200  $\mu\text{A}$ , producing a power density of 30  $\text{W}/\text{cm}^2$ . The strain profile induced by the implant and after subsequent annealing was then investigated with a Bede D3 high-resolution X-ray diffractometer in double-axis diffraction mode (DAD). The defect structure of the implanted region was imaged by cross-sectional transmission electron microscopy (XTEM) after annealing.

Additional implanted pieces from each run were bonded to GaAs handle wafers to investigate the exfoliated layers. The GaAs handle wafers were coated with 800 Å of SiN and outgassed at 500°C for 1 min in nitrogen. The bonding was carried out in air at room temperature using an oxygen plasma surface activation (200 mW, 200 mTorr) followed by a DI water rinse and nitrogen dry. The bond was strengthened by annealing for 3 h at 150°C, at which point the temperature was increased to 300°C to induce the exfoliation of the InP layer.

## 3. Results

The double-axis X-ray  $\omega/2\theta$  scans for the doses of  $2.5 \times 10^{16}$  and  $5.0 \times 10^{16} \text{H}_2^+/\text{cm}^2$  are shown in Fig. 1. Figure 1(a) shows both doses where the target was not cooled. These scans show a compressively strained layer, with some distribution of strain, to the left of

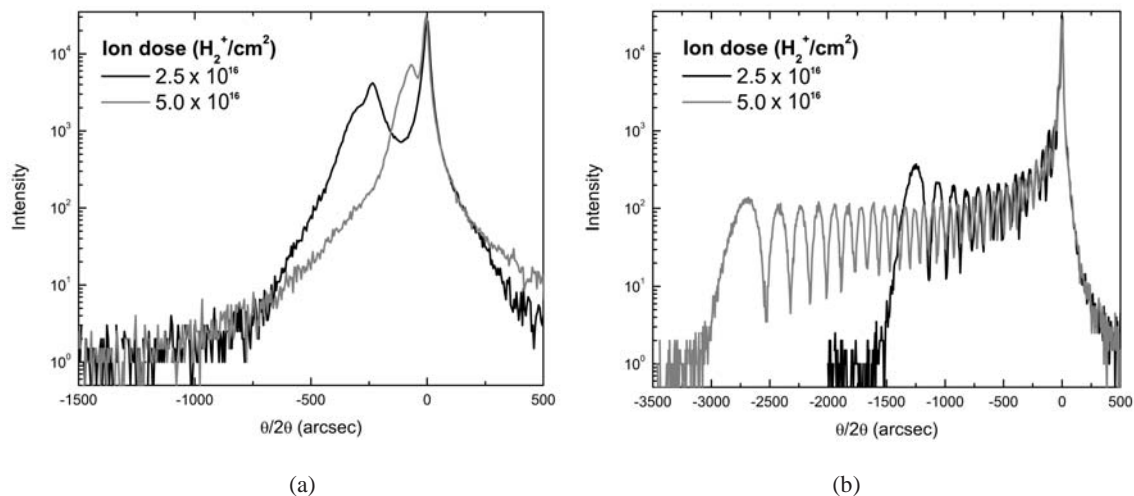


Fig. 1. 004 DAD X-ray  $\theta/2\theta$  scans of as-implanted InP for various doses: (a) implantation at room temperature and (b) implantation at nominally  $-20^\circ\text{C}$ .

the substrate peak, which is induced by the implantation. In contrast, Fig. 1(b) shows the DAD  $\theta/2\theta$  scans for equivalent doses where the InP substrate was cooled to  $-20^\circ\text{C}$ . In this as-implanted case, the strain presents itself as a set of fringes to the left of the substrate peak. This curve can be computer simulated (Bede RADS Mercury) very accurately with a modified Gaussian strain distribution. The dose in the cooled sample has a 1:1 relationship with the maximum amount of strain detected by X-ray diffraction,  $2.5 \times 10^{16} \text{ H}_2^+/\text{cm}^2$  having a maximum strain of 1% and  $5 \times 10^{16} \text{ H}_2^+/\text{cm}^2$  having a maximum strain of 2%. In the case of the uncooled implantation, the dose is actually inversely related to the amount of strain,  $2.5 \times 10^{16} \text{ H}_2^+/\text{cm}^2$  having a maximum strain of 0.1% and  $5 \times 10^{16} \text{ H}_2^+/\text{cm}^2$  having a maximum strain of 0.02%.

Figures 2(a) and 2(b) show the strain profile of the implanted samples after various annealing temperatures. The samples were annealed at  $150^\circ\text{C}$  and  $300^\circ\text{C}$  for 1 h each. The samples implanted at  $-20^\circ\text{C}$  and annealed at  $300^\circ\text{C}$  resembled the as-implanted profiles that were not cooled during the implantation, indicating that the uncooled, implanted samples exhibited significant heating during the implantation step. In general, the strain from the implant is reduced with annealing where higher annealing temperature accelerates the strain relaxation. However, the strain profile for the uncooled InP changes very little with annealing, while the cooled InP exhibits significant strain relaxation; *e.g.*, after  $150^\circ\text{C}$  annealing the uncooled InP shows negligible strain relaxation whereas the cooled InP relaxes from 2% to 0.9% strain.

The damaged structures of the InP implanted at room temperature and at  $-20^\circ\text{C}$  are shown in the XTEM images of Figs. 3(a) and 3(b), respectively. It is evident that the damage profile in the room-temperature sample, which consists of a high density of small dislocation loops, is quite large and extends from the projected range of 700 nm to the surface of the substrate. In contrast, the defects of the cooled sample are well confined to

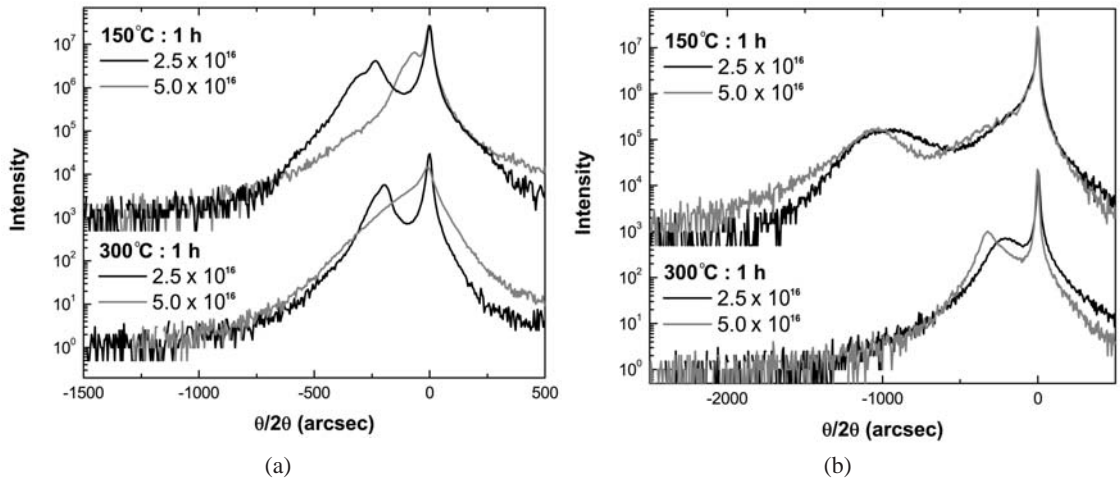


Fig. 2. 004 DAD X-ray  $\theta/2\theta$  scans of implanted InP annealed at various temperatures: (a) implantation at room temperature and (b) implantation at nominally  $-20^\circ\text{C}$ .

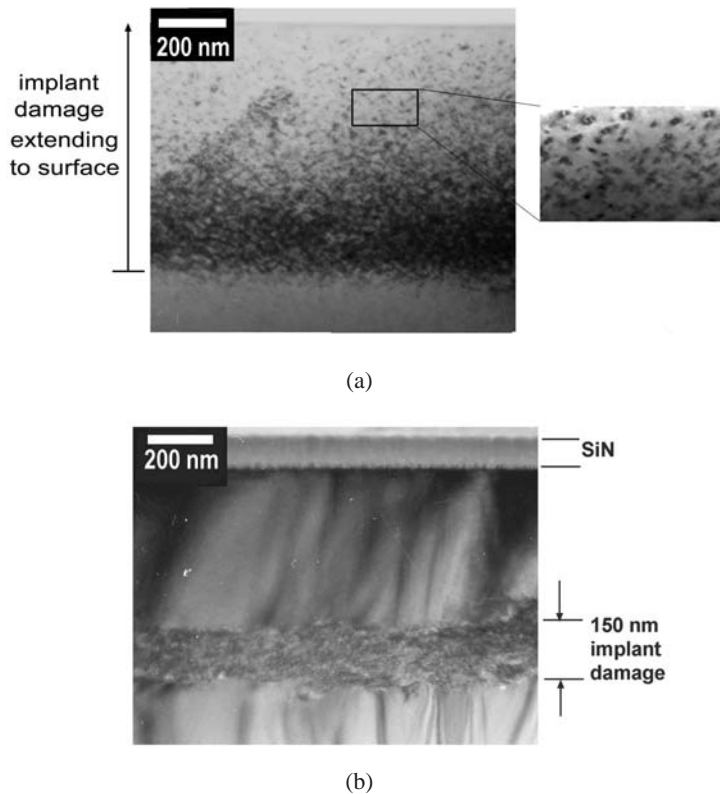


Fig. 3. Cross-sectional TEM images of implanted InP annealed at  $150^\circ\text{C}$  for 1 h: (a) implantation at room temperature and (b) implantation at  $-20^\circ\text{C}$ .

a single layer at the projected range with a width of 150 nm (which is only slightly larger than the predicted straggle of  $\sim 100$  nm).

As-implanted samples with a dose of  $5 \times 10^{16}$   $\text{H}_2^+/\text{cm}^2$  of both the uncooled and cooled implantation conditions were bonded to GaAs handle wafers and the layer transferred. No exfoliation occurred during the  $150^\circ\text{C}$  bond strengthening annealing step. The cooled sample produced exfoliation within a few seconds of increasing the temperature to  $300^\circ\text{C}$ , while the uncooled sample did not exfoliate even after increasing the temperature to  $500^\circ\text{C}$ . Figure 4(a) shows an atomic force microscopy image of the transferred InP layer from the sample that was cooled during implantation. The roughness of the as-split layer is  $\sim 80$  nm. The thickness of the layer is  $\sim 0.7$   $\mu\text{m}$  and, as can be observed in Fig. 4(b), the cleavage occurred near the end of the damaged region that is imaged by cross-sectional TEM.

#### 4. Discussion

As ions are implanted into the lattice, a defective region including interstitial hydrogen/molecular hydrogen, self-interstitials, vacancies, and various hydrogen complexes is formed at the projected range. Some of these defects will introduce strain in the lattice producing the strain profiles shown in the X-ray data. A compressively strained layer was previously observed after the implantation of a variety of semiconductor materials<sup>(9,10)</sup> and has been interpreted as point-defect-induced tetragonal distortion.<sup>(10)</sup> For the cooled ( $-20^\circ\text{C}$ ) specimen, this strain manifests into a Gaussian-like distribution which is expected from an as-implanted ion distribution,<sup>(11)</sup> indicating that during implantation the ions are not mobile. Additionally, since the amount of strain and the dose show a 1:1 correlation for cooled implantation conditions, it may be concluded that the level of strain is a good indicator of the as-implanted ion concentration.<sup>(12,13)</sup> As the implanted material is annealed, diffusion and agglomeration of the point defects occur and relaxes the strain, as shown in Fig. 2.

It is known that the implantation itself induces heating of the wafer so that if the material is not actively cooled, the implantation is performed at a temperature higher than

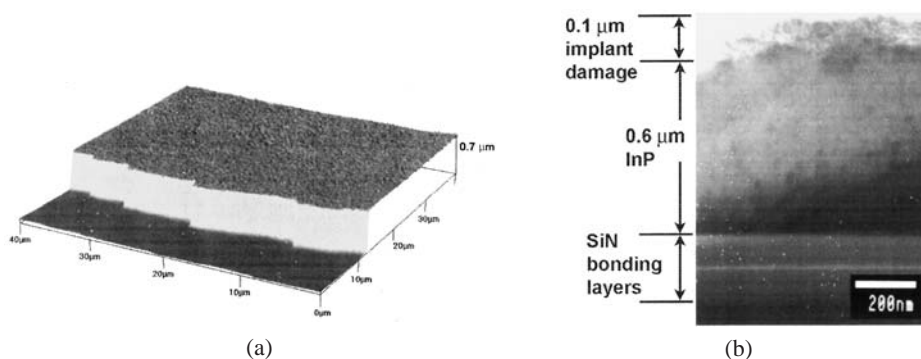


Fig. 4. (a) AFM of transferred InP layer on GaAs substrate and (b) cross-sectional TEM image of transferred InP layer.

room temperature.<sup>(14,15)</sup> Therefore, it is expected that some of the defects anneal out during the implantation. In the case of the uncooled InP, it appears that the temperature of the sample may have approached 300°C (as the strain profile is similar to that of the cooled sample that was subsequently annealed at 300°C). These temperatures are in agreement with previous calculations of implantation-induced heating where for GaAs with a similar power density the temperature was expected to reach 200°C.<sup>(15)</sup> Additionally, for the uncooled implant, the maximum as-implanted strain is inversely related to the dose. If the heating of the sample is proportional to the dose,<sup>(14)</sup> then for a higher dose more defects can be annealed out during the implantation, causing a further reduction in strain. These implants exhibit less strain relaxation after subsequent annealing possibly because the metastable state of the as-implanted structure has already been relieved by implantation-induced heating. The defect structure of the uncooled sample shows a high density of secondary implantation defects, i.e., Frank dislocation loops. These are known to form from the diffusion and agglomeration of point defects<sup>(11)</sup> and are able to form simultaneously during implantation if the implantation is carried out at higher temperatures.<sup>(16)</sup>

Exfoliation occurs by the agglomeration of hydrogen into plateletlike defects, which eventually coalesce to exfoliate the layer. To form these defects the lattice must effectively trap the hydrogen, which is thought to occur in a particular temperature regime.<sup>(6,7)</sup> In the uncooled InP specimen, the temperature reached well above the previously reported temperature window.<sup>(6)</sup> The failure to exfoliate the layer in this case can then be attributed to the loss of hydrogen and the inability to form platelet-type defects at a localized depth. Additionally, it has been reported that exfoliation is influenced by the depth of the maximum damage;<sup>(8)</sup> therefore, since the damage in the uncooled InP is widely distributed, the hydrogen may not be able to agglomerate within a sufficiently narrow thickness to exfoliate the layer. The relatively thin highly damaged region shown in the cooled, implanted InP may be able to trap more effectively the hydrogen allowing greater coalescence of the hydrogen and the platelet defects.

While exfoliation in Si has been found to be quite robust, producing exfoliation for a wide variety of implantation parameters,<sup>(8,17)</sup> this does not appear to be the case for III-V materials. First, III-V materials exhibit inferior mechanical strength; therefore ion implantation damage may play a critical role in the quality of these transferred layers. Secondly, III-V materials display a significantly lower thermal conductivity than Si (*e.g.*, InP ~ 0.68 W/cm°C, and Si ~ 1.3 W/cm°C), which will ultimately lead to greater target heating during implantation. Because it has been found that the exfoliation of III-V materials lies within a smaller implantation temperature range,<sup>(6)</sup> it is critical to control this parameter. The temperature experienced by the target will depend upon a variety of factors, including beam power density, ion dose, thermal conductivity of the target, as well as how the wafer is affixed during the implantation.<sup>(14,15)</sup> Therefore, these factors must be optimized to minimize any uncontrolled temperature excursions during the processing of III-V materials and we have found that actively cooling InP substrates to -20°C during implantation is sufficient to produce successful exfoliation.

## 5. Conclusions

Since III-V materials exhibit a significantly lower thermal conductivity than Si, target heating due to the implantation process is a critical concern. In this study, InP implanted without cooling did not produce exfoliation due to the loss of hydrogen and the inability to form localized platelet-type defects during subsequent higher (150°C then 300°C) temperatures. Additionally, the damage profile in the InP implanted without cooling is quite large and extends all the way to the surface of the substrate, while the defects of cooled (−20°C) InP are confined to a single layer with a thickness of 150 nm at the projected range. The relatively thin highly damaged region shown in the low-temperature-implanted material is speculated to trap more effectively the hydrogen allowing more efficient coalescence of the hydrogen and the platelet defects. We have achieved temperature control through sample cooling; however, altering the implant parameters (dose rate, etc.) to maintain a low sample temperature should also promote successful exfoliation during subsequent annealing.

## Acknowledgements

This work was supported by DARPA ABCS (through Northrop Grumman Space Technology) and the National Science Foundation (DMR-0408715).

## References

- 1 A. F. i. Morral, J. M. Zahler, H. A. Atwater, S. P. Ahrenkiel and M. W. Wanlass: *Appl. Phys. Lett.* **26** (2003) 5413.
- 2 K. D. Hobart and F. J. Kub: *Electron. Lett.* **35** (1999) 675.
- 3 M. Bruel: *Electron. Lett.* **31** (1995) 1201.
- 4 M. K. Weldon, V. E. Marsico, Y. J. Chabal, A. Agarwal, D. J. Eaglesham, J. Sapjeta, W. L. Brown, D. C. Jacobson, Y. Caudano, S. B. Christman and E. E. Chaban: *J. Vac. Sci. & Technol. B* **15** (1997) 1065.
- 5 I. Radu, I. Szafraniak, R. Scholz, M. Alexe and U. Gösele: *Int. Semiconductor Conf. CAS 2002 Proc.* (2002) p. 305.
- 6 Q. -Y. Tong, L. J. Huang and U. Gösele: *J. Electron. Mater.* **29** (2000) 928.
- 7 S. Hayashi, D. Bruno and M. S. Goorsky: *Appl. Phys. Lett.* **85** (2004) 236.
- 8 J. K. Lee, M. Nastasi, N. D. Theodore, A. Smalley, T. L. Alford, J. W. Mayer, M. Cai and S. S. Lau: *J. Appl. Phys.* **96** (2004) 280.
- 9 S. Lombardo, K. K. Larsen, V. Raineri, F. L. Via and S. U. Campisano: *J. Appl. Phys.* **79** (1996) 3456.
- 10 S. T. Horng and M. S. Goorsky: *Appl. Phys. Lett.* **68** (1996) 1537.
- 11 S. K. Ghandhi: *VSLI Fabrication Principles* (John Wiley & Sons Inc., New York, 1994).
- 12 C. Bocchi, P. Franzosi, L. Lazzarini and G. Salviati: *J. Electrochem. Soc.* **140** (1993) 2034.
- 13 C. Miclaus and M. S. Goorsky: *Journal of Physics D: Appl. Phys.* **36 A** (2003) 177.
- 14 P. D. Parry: *J. Vac. Sci. & Technol.* **3** (1976) 622.
- 15 I. Radu: *PhD Dissertation, Martin-Luther Universitat Halle-Wittenberg* (2003).
- 16 Y. Gao, S. P. Wong, W. Y. Cheung, G. Shao and K. P. Homewood: *Appl. Phys. Lett.* **83** (2003) 42.
- 17 Q. -Y. Tong and U. Gösele: *Semiconductor Wafer Bonding* (John Wiley and Sons Inc., New York, 1999).